# Electronic Supplementary Information

# Facile fabrication of micro-/nanostructured, superhydrophobic membranes with adjustable porosity by 3D Printing

Fadoua Mayoussi[a], Egan Doeven[d], Andrea Kick[a], Andreas Goralczyk[a], Yi Thomann[b,c], Patrick Risch[a], Rosanne M. Guijt[d], Frederik Kotz[a,b], Dorothea Helmer*[a,b,c] and Bastian E. Rapp[a,b,c]

[a] Laboratory of Process Technology | NeptunLab, Albert-Ludwigs University Freiburg, Department of Microsystems Engineering (IMTEK), Georges-Köhler-Allee 103, Freiburg, Germany.

[b] Freiburg Materials Research Center (FMF), Albert-Ludwigs-University Freiburg, Freiburg, Germany.

[c] FIT Freiburg Centre for Interactive Materials and Bioinspired Technologies, Albert-Ludwigs University, Freiburg, Germany

[d] Deakin University, Centre for Regional and Rural Futures, Geelong, VIC, 3220, Australia.

Table S1: the linear shrinkage of the membranes after the porogen removal

| | **Shrinkage (%)** | |
|---|---|---|
| | x-y direction | z direction |
| **Fluoropor 15** | 20 | 32 |
| **Fluoropor 25** | 14 | 26 |

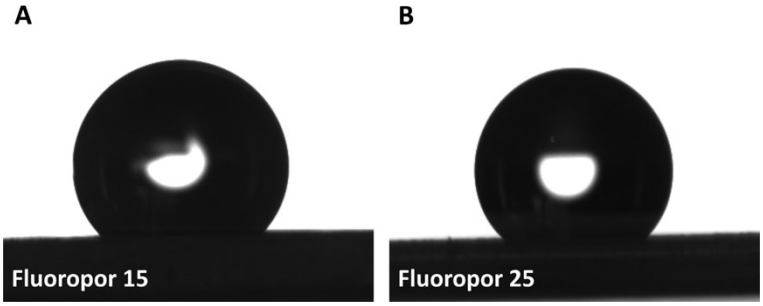


Figure S 1: Image of the water contact angle on top surface of both membranes. Fluoropor 15 membrane shows a static contact angle of 123±2 °, whereas Fluoropor 25 membrane shows a static contact angle of 126±4 °. The top surface of the directly printed membranes show a lack of porosity because of their direct contact to the printer's bath foil during the print.

**Image analysis for the determination of the pore size distribution**

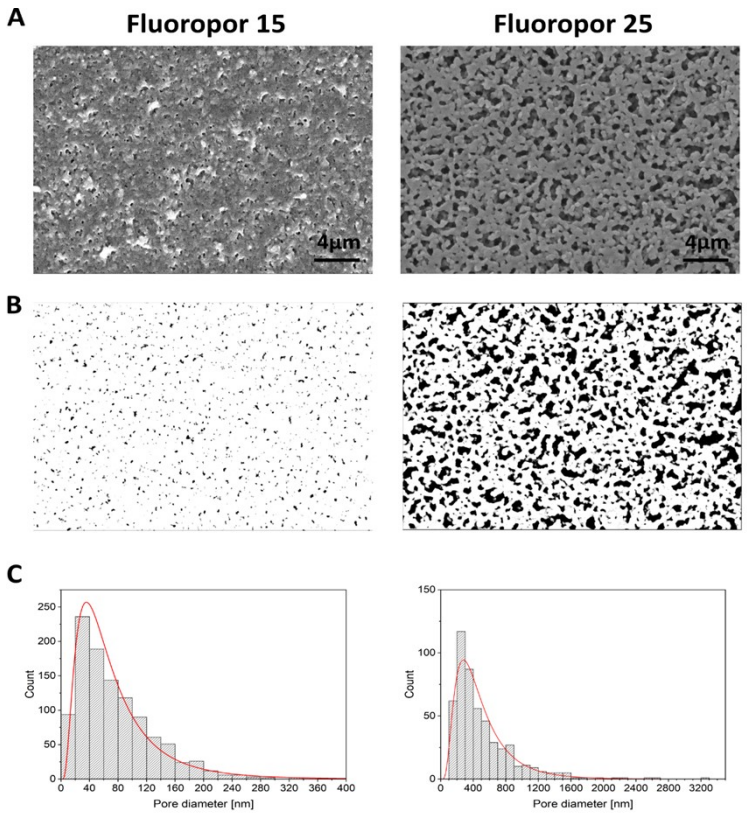


Figure S 2: Pore size distribution of the printed Fluoropor stack membranes. A) The SEM images of cross sectioned areas with a slice thickness of 1µm cut by using a cryo-ultramicrotome at -120 °C. B) Binarized images, generated from the original image by thresholding. C) Plotted pore size distribution of both Fluoropor 15 and Fluoropor 25 membranes.

**Determination of the water content in the separated oils**

To evaluate the separation capability of the membranes and the purity of the collected oils, anhydrous copper sulfate (500 mg) was added after the separation to detect water content. Anhydrous copper sulfate changes color in contact with water from white to blue. After adding it to the mixture, no change in color was detected confirming the purity of the collected oils.

To validate this procedure, we performed reference experiments with samples of four different volume ratios of chloroform-water (see Table S.2). Anhydrous copper sulfate was added to the mixtures to detect the water in the mixture. Figure S. 5 shows that anhydrous copper sulfate can detect water even at concentrations as low as 0.01 vol%. This suggests that the residual water-in-oil after extraction was below this threshold.

Table 2: the required volumes of chloroform and water for the preparation of the mixtures. The amount of water in the mixture is given in Vol%

| Mixture | $V_{chloroform}$ (ml) | $V_{water}$ (µl) | Water content (Vol %) |
|---|---|---|---|
| **1** | 6 | 600 | 10 |
| **2** | 6 | 60 | 1 |
| **3** | 6 | 6 | 0.1 |
| **4** | 6 | 0.6 | 0.01 |

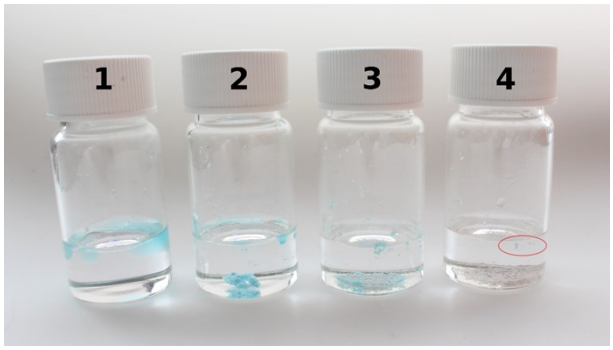


Figure S 3: Detection of water traces in oil/water mixtures by anhydrous copper sulfate. Photograph of chloroform-water mixtures with different ratios. The added anhydrous copper sulfate (white color) changes to a blue color when in contact with water. The anhydrous copper sulfate can detect water even at very small concentrations (0.01 vol %).

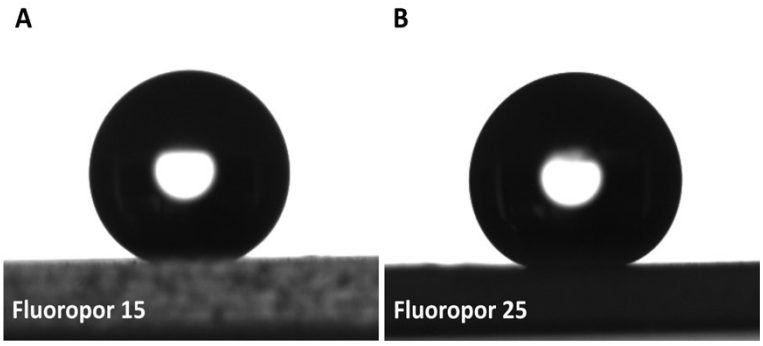


Figure S 4: Images of the water contact angle on top of the peeled superhydrophobic membranes. The membranes show a static contact angle 161±2 ° and 164±7 ° for Fluoropor 15 (A) and Fluoropor 25 (B) membranes, respectively. The water droplet is completely repelled by both surfaces.

**Investigation of the mechanical properties of the thin superhydrophobic membranes:**

The mechanical strength of the peeled superhydrophobic membranes is shown in Figure S 5. The point of rupture was measured to be 22 ± 4 % strain for Fluoropor 15 and 32 ± 1% strain for Fluoropor 25 (See Figure S 5). It can be observed that the force needed to stretch Fluoropor 15 membrane is higher in comparison to Fluoropor 25 membrane, which is also shown in Table S 2 with the higher value of the elastic modulus.

Table S2: The measured elastic modulus of the thin superhydrophobic membranes

| | **Fluoropor 15** | **Fluoropor 25** |
|---|---|---|
| **Elastic modulus (MPa)** | 52 ± 6 | 18 ± 1 |

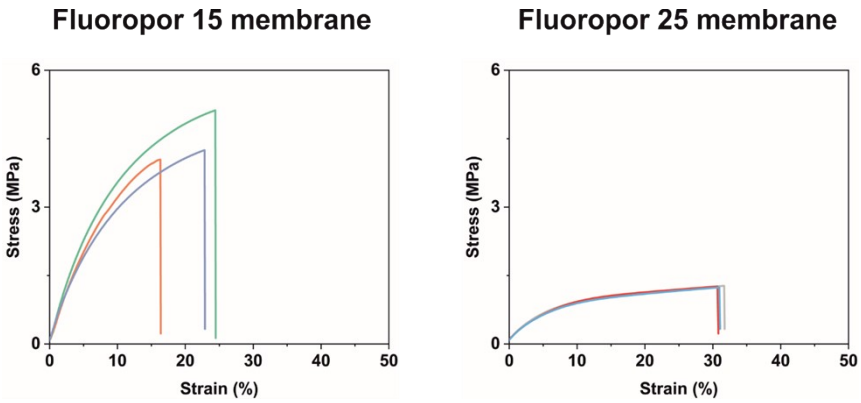


Figure S 5: Stress-strain curves of the peeled superhydrophobic membranes